NATIONAL ADVISORY COMMITTEE FOR AERONAUTICS

TECHNICAL NOTE 4215

APPLICATION OF A HIGH-TEMPERATURE STATIC STRAIN GAGE TO THE MEASUREMENT OF THERMAL STRESSES IN A TURBINE STATOR VANE

By R. H. Kemp, C. R. Morse, and M. H. Hirschberg

Lewis Flight Propulsion Laboratory
Cleveland, Ohio

NACA

Washington
March 1958

NATIONAL ADVISORY COMMITTEE FOR AERONAUTICS

TECHNICAL NOTE 4215

APPLICATION OF A HIGH-TEMPERATURE STATIC STRAIN GAGE TO THE MEASUREMENT OF THERMAL STRESSES IN A TURBINE STATOR VANE

By R. H. Kemp, C. R. Morse, and M. H. Hirschberg

SUMMARY

The thermal stresses in a turbine stator vane of a turbojet engine were measured by means of static high-temperature resistance-wire strain gages. The temperature variations existing in the engine were duplicated in the vane in a test setup at a reduced average temperature. Stress measurements at the leading and trailing edges indicated maximum principal values in compression of 18,100 and 27,200 psi, respectively. In the midchord region on the suction surface, the maximum principal stress was 19,600 psi in compression and in the midchord region on the pressure surface, 26,200 psi in tension.

The high-temperature strain gage developed for measuring the static strains was satisfactory up to 800° F. Karma is used as the strain-sensitive element and is bonded to the test structure with Quigley 1925 ceramic coating. The gage factor for a 1/4- by 1/4-inch gage was 2.16 at room temperature and 1.93 at 800° F. Shift of the zero point was below 1.2 microinches per inch per hour at temperatures under 600° F. At 750° F, the zero shift was 5.8 microinches per inch per hour.

INTRODUCTION

The turbine stator vanes of a turbojet engine are subjected to cyclic thermal stresses as a result of cyclic temperature distributions throughout the vane occurring in both transient and steady-state conditions of engine operation. Transient variations or distributions of temperature occur at start, during acceleration and deceleration, and when the engine is stopped. During steady-state operation of the engine, temperature variations also occur in the vane as a function of combustion-gas temperature distribution, heat conduction and radiation paths, and cooling air forced through the hollow vanes.

As a first approach to a determination of the magnitude of the stresses resulting from the temperature variations, a research program was undertaken at the Lewis Flight Propulsion Laboratory to investigate the steady-state condition. To facilitate the measurements of the thermal stresses, the temperature variations as measured in the engine under steady-state conditions were duplicated in a sample vane in a bench test setup. In addition, since the stress distribution is not affected by a change in the average temperature, the test conditions were imposed at a decreased average temperature, thereby making it possible to use static high-temperature resistance-wire strain gages developed during the investigation.

The measurement of static strains at elevated temperatures (temperatures above 200° F) has posed a very serious problem in many fields of research. Where the gage length can be made relatively long (1 in. or more), it has been possible to obtain strain information with techniques involving optical methods or probes attached at the gage points, leading to some type of measuring device at room temperature. The strain values obtained are, therefore, the average strain over a considerable length and involve, in general, rather cumbersome equipment, limiting severely the number of locations at which measurements can be made.

In reference 1 during a research program involving the development of a high-temperature strain gage for dynamic use, Karma displayed a low-temperature coefficient of resistance over a range of temperatures up to 800° or 900° F. This physical characteristic has been utilized in a study at the Lewis laboratory to employ the Karma wire as the sensing element of a high-temperature static strain gage. The principal advantages lie in the small gage length which can be obtained and in the increased number of measurement positions which become practical. In addition, the ability to record the strain at a remote location is valuable in many cases.

This report describes the high-temperature static strain gage and presents the results obtained in a determination of the thermal stresses in a turbine stator vane resulting from the temperature distribution obtained under steady-state conditions at rated speed and temperature of the engine.

SYMBOLS

The following symbols are used in this report:

A	cross-sectional area
C_1, C_2, C_3	coefficients

E	elastic modulus
I	moment of inertia, $in.^4$
i	individual area
K	strain-gage sensitivity factor
n	total number of finite areas
R	resistance
r	radius, in.
T	temperature, ^oF
t	thickness, in.
x,y,z	coordinate axes
α	coefficient of thermal expansion, ^oF
ε	strain, microin./in.
σ	stress, psi

STATIC HIGH-TEMPERATURE STRAIN GAGE

Requirements for a Resistance-Wire Static Gage at Elevated Temperatures

The physical properties of resistance-wire strain gages used for measurements at elevated temperatures must remain stable and within narrow limits up to the temperature at which the strain measurement is made. For example, the wire-sensing element should have the following characteristics:

(1) Low and stable temperature coefficient of resistance over the temperature range

(2) High and stable specific resistivity

(3) High resistance to corrosion or surface-film changes

(4) High degree of metallurgical stability

(5) Metallurgical condition amenable to fabrication into grids

The actual coefficient values and degrees of stability which must be attained depend largely on the accuracy desired in the strain measurements, the length of the time period over which the measurements must be taken, and the magnitude and character of the temperature variations that occur at the gage location during the test.

Previously in this report, the resistance-wire element itself was discussed. Now the requirements which must be met by the material that bonds the wire element to the specimen surface must also be considered. The adhesion must be sufficient to permit good strain transference from the specimen to the wire at all the strains and temperatures encountered. The bonding material must be free of creep at all the strain, time, and temperature values encountered and must provide a noncorrosive environment for the wire, have a low electrical conductivity at all temperatures, and be in a form amenable to the mounting technique required. All of the previously noted requirements enter into a final determination of the over-all suitability of a particular combination of components for measuring static strains at elevated temperatures.

Obviously, satisfaction of all of the stated requirements with presently available materials presents a most formidable problem. By sacrificing maximum temperature of operation, for example, a static high-temperature strain gage can be obtained through the use of proper techniques, which will be at least a partial solution to the over-all problem. The static high-temperature strain gage described in this report must be regarded as part of this solution. One of its limitations, for example, is a maximum operating temperature of approximately 800° F.

Materials for Static High-Temperature Strain Gage

Karma was the wire alloy chosen for the strain-sensing element on the basis of previous research (ref. 1). Reference 1 shows in a comparison of the temperature coefficients of resistance of the wire alloys 80-percent platinum - 20-percent iridium, Nichrome V, Advance and Karma, that the Karma wire in the as-received condition has a temperature coefficient (100° to 800° F) comparable with that of Advance. The temperature coefficients are presented in table I in terms of apparent strain per °F. The values shown were obtained from sample gages mounted on HS-21 alloy bars and should be considered only as approximate values since wire from other batches will display somewhat different characteristics. An error of 1° in the determination of the gage-wire temperature would cause an error of 900 psi in the case of Nichrome V and an error of 2400 psi in the case of the platinum-iridium alloy if these wires were to be used in static strain gages. Karma, on the other hand, would result in an error of only 75 psi. The use of Advance for elevated temperatures is,

of course, restricted by its poor oxidation resistance. Another advantage of Karma lies in its high specific resistivity (table I) of approximately 800 ohms per circular mil foot which permits higher signal levels to be obtained.

Karma wire is also used for the lead-wire material because of its low-temperature coefficient of resistance. This property outweighs the disadvantage of its higher resistivity when compared with such materials as nickel or platinum. The leads are divided into the following two parts: A primary lead of 0.010-inch Karma approximately 1/2 inch long is fastened to the 0.001-inch strain-sensitive wire and serves as an intermediate connection to the secondary lead. The secondary lead of 0.025-inch Karma is carried out of the hot region to room-temperature environment. Conversion is then made to copper for connection to the instrumentation.

The bonding material for both the precoat and covercoat is the high-temperature Quigley 1925 ceramic coating. This material is baked at 600° F, which does not exceed the temperature limit of the wire. In cases where the specimen can be heated to a higher temperature, a 0.002-inch precoat, designated L-6AC ceramic by the National Bureau of Standards and fired at 1750° F, is preferred. The L-6AC provides an excellent base for the Quigley 1925 covercoat.

When Quigley 1925 is used, two modifications are necessary to produce the required results. First, it was necessary to mill the as-received material in a procelain ball mill for 48 hours using procelain balls. This reduced the particle size sufficiently to prevent interference with the 0.001-inch wires when mounting. In addition, inconsistent results were obtained when material from various batches was used. This inconsistency manifested itself in the form of hardness, adhesion variations, and tendencies for crazing or cracking. The pH, determined with glass electrodes, of mixtures which have given satisfactory results, was approximately 1.6. The phosphoric acid concentration was critical in affecting these properties. When the acid concentration was deficient, the ceramic after baking was soft, had little resistance to abrasion, and had poor adhesion. When the phosphoric acid concentration was too high, the cement was very hard and tended to form a network of hairline cracks. Upon experimentation, it was determined that each deficient batch could be modified by phosphoric acid additions to produce a baked material having more or less optimum properties of good adhesion, ample hardness, and resistance to abrasion and cracking.

Gage Grid Construction

Several different methods of construction of the sensing elements have been employed. One of these is similar to the method described in reference 1 and is illustrated in figure 1. A stain-sensitive filament is first prepared by attaching 0.010-inch Karma lead wires to a suitable length of 0.001-inch Karma wire. The attachment may be made by welding,

tube-tipped lead described in reference 1. The filament is wound around two rods held against the mounting frame by a second frame, and the lead wires are inserted in their respective holders. This stage of fabrication is illustrated in figure 1(a). The gage length can be varied from 1/8 inch to 5/8 inch with one set of frames. Each loop of the grid is tied to the mounting frame with a single strand of silk thread, and the rods and rod-carrying frame are removed. The strain-sensitive grid is then ready for mounting as shown in figure 1(b).

A second method of preparing the grid, which has been used extensively at the Lewis laboratory, involves a jig shown in figure 2. The jig consists of three blocks of hardened steel, one of which has 0.025-inch-diameter pins inserted in holes which pass completely through the block. The pins are spaced to permit the forming of a wire grid of the required dimensions and resistance. After winding the strain-sensitive wire around the pins as shown in figure 2, the plain block is placed on top of the grid, and the block containing the relief slots is placed below the one on which the grid is wound. The stack of three blocks is then placed in a press and pressure applied. The pins move down through their respective holes and protrude into the slots in the relief block. The plain block moves into contact with the grid and deforms the wire depending on the pressure applied. The cold working of the wire stabilizes the grid shape and permits direct handling. Several modifications may be employed at this stage. For example, with only minor amounts of cold working (approximately, 5- to 10-percent reduction in diameter), a strip of masking tape 1/16 to 1/8 inch wide may be placed on the grid between the two rows of pins, and then the grid is removed and handled by the tape strip with a pair of tweezers. With greater amounts of cold work (approximately, 20- to 30-percent reduction in diameter), the dimensionally stabilized grid itself may be handled with tweezers without a tape strip.

4715

Gage Mounting Techniques

A 0.002- to 0.004-inch precoat of the modified Quigley 1925 is sprayed on the prepared specimen surface using an artists air brush. Spraying produces more uniform and more readily controlled thicknesses than brushing. The precoat after drying several hours at 150° F is baked at 600° F for one-half hour.

When using the grid prepared in the mounting frame, the frame is placed in position on the specimen surface with the grid in contact with the precoat. A thin coat of cement is applied to the grid area leaving the loop ends uncovered. After drying at 150° F for 1 hour, the threads can be cut and removed together with the frame. A second coat of cement is applied, covering the entire installation, and is baked at 600° F for one-half hour after drying several hours at 150° F.

When using a pressure stabilized grid, the grid is placed in position and held by means of strands of thread taped in place across the grid or by thin strips (1/32 inch wide) of masking tape placed across the grid ends. A thin coat of cement is applied to the grid (not on thread or tape) and baked. The threads or tape are then removed, and a second coat of cement applied and baked. Tube-tipped leads or welded leads may be attached before or after the central portion of the grid is covered with cement. Both methods have been used satisfactorily.

4715

Gage Characteristics

Initial stabilization. - After the final baking of the completed gage installation at 600° F for one hour, the gage can be used for strain measurements. In static applications, however, it is found that considerable zero shift inevitably occurs, generally in an erratic manner. This erratic shift continues to occur for as many as 50 hours after the gage is put into operation. There are three predominant factors which produce this phenomenon. (1) The chemical reactions which occur in the cement during the baking cycles probably do not go to completion or equilibrium for some time after the gage is placed in operation. This could result in small dimensional changes in the cement and hence affect the gage resistance. (2) Considerable time is probably required to establish a stable film on the surface of the wire. (3) Considerable time may be necessary to establish stable or equilibrium values of specific resistivity and temperature coefficient.

An indication of the extreme dependence of the zero shift on the surface film may be obtained by computing the thickness of a layer of metal which would have to be removed from the surface of a 1-mil wire to produce, for example, a change in indicated strain of 100 microinches per inch. It can readily be shown that the thickness t of a surface layer which would have to be removed to produce a given indicated strain change is

$$t = -\frac{rK\varepsilon}{2}$$

where r is the radius of the wire, K is the strain-sensitivity factor of the wire, and ε is the indicated strain change. A change of 100 microinches per inch indicated strain would therefore be obtained with the removal of a surface layer only 5×10^{-8} inches thick. It is, therefore, necessary to produce a stable film and to obtain environmental conditions which will not alter it. Tests of a large number of gages have indicated that after approximately 50 hours of operation at temperatures in the neighborhood of 700° to 750° F, the zero shift becomes stabilized at relatively low and consistent values. As a result, a soaking period at 700° to 750° F of at least 50 hours is used for all new gage installations

before attempting to make static strain measurements. Additional information concerning the zero shift after this period is presented later in this report.

Short time characteristics of static strain gage. - The variation of resistance with temperature for a completely installed Karma gage is shown in figure 3. As the temperature is increased, the resistance changes by only a small amount, until approximately 900° F is reached. At this temperature a metallurgical change takes place in the wire, and the resistance drops rapidly. On cooling to room temperature and on subsequent cycles of heating and cooling, the lower curve is traversed. It is the characteristic flat portion of the curve up to approximately 800° F which is utilized in making static strain measurements. Practical use of the flat portion of the curve above 800° F and up to 1000° F (fig. 3) is not recommended unless accuracy is to be sacrificed, because the actual position of the knee of the curve is a time-temperature function. At longer times, for example, the knee effectively moves to the left on the temperature scale. This will be discussed further in the section on long time characteristics.

Since the ordinate of figure 3 is highly compressed in terms of customary values of strain, an expanded scale is used in figure 4 to show the resistance variation of Karma in the as-received condition up to 800° F when mounted as gages on two different alloys, S-816 and HS-21. These curves indicate resistance changes in terms of equivalent strain of approximately 1700 and 1050 microinches per inch for HS-21 and S-816, respectively, in the temperature range of 100° to 800° F. The difference between the two curves is due to the difference in the expansion coefficients of the two alloys. The magnitude of the resistance changes is sufficiently small to permit reasonably accurate corrections from gage temperature determinations with thermocouples and isothermal calibration curves for each gage.

The gage sensitivity factor and its variation with temperature for the Karma gages was measured in a static constant-bending-moment apparatus. An Inconel bar was used for the constant-bending-moment beam and was surrounded by a furnace to permit heating of the gages to any desired temperature. The beam was loaded to a stress of 25,000 psi at the gage locations with checkpoints taken at intermediate values to establish the fact that the gages were responding linearly with load. The following three different gage sizes were investigated together with the nominal resistances obtained in each size configuration:

(1) 1/16 Inch wide by 3/8-inch gage length; 95 ohms

(2) 5/32 Inch wide by 5/32-inch gage length; 115 ohms

(3) 1/4 Inch wide by 1/4-inch gage length; 200 ohms

The results of the gage factor determinations are shown in figure 5. The 1/4x1/4 and 5/32x5/32 gages have a gage factor of 2.16 at room temperature which drops to approximately 1.93 at 800° F. The 1/16x3/8 gage shows a higher gage factor (2.28 at room temperature) resulting from the lower cross sensitivity of this configuration.

The information presented concerning gage factors and other characteristics was obtained from a limited number of gages fabricated from specific batches of wire. As workers in the strain-gage field know, the characteristics may vary considerably among batches of wire and even change along the length of a given piece of wire from one spool. Therefore, the exact numbers quoted herein should not be used as constants but should rather be treated as approximate values.

Long time characteristics of static strain gage. - In addition to the short time characteristics of resistance and gage-factor variation with temperature, there is the additional problem of changes with time. These changes can either be involved in wire surface-layer changes or in internal metallurgical changes which in turn cause changes in specific resistivity, temperature coefficient of resistance, and other related constants. An unknown change in these quantities, of course, results in a loss of the initial reference zero point and hence invalidates additional readings.

To obtain some indication of the order of magnitude of these long time changes, gages were mounted on annealed bars of S-816 and placed in a furnace with no load applied. The strain gages were connected to static bridge equipment, and the bridges were balanced or zeroed. A running check was then kept of the zero shift with time while the temperature was held constant at various levels. In all cases, the zero shift was erratic during the first hours of operation, as noted previously. After 50 hours at temperature, the erratic nature of the zero shift disappeared, and up to 800° F the resistance change was then linear with time. In figure 6, the zero shift is plotted against time in days after stabilization has occurred for temperatures of 600°, 700°, and 750° F. The resistance change or zero shift is linear with time, and the rate of change of resistance increases with temperature. At 600° F, the rate of change is 1.23 microinches per inch per hour; at 700° F, the two gages give an average of 2.76 microinches per inch per hour; and at 750° F, the two gages give an average of 5.83 microinches per inch per hour. The increase in the rate of change of resistance is probably predominantly a result of an increased rate of corrosion with increasing temperature.

At 800° F the zero shift no longer occurs in the same manner as already indicated for the lower temperatures. Figure 7 shows the zero shift of two gages at 800° F which have previously undergone stabilization treatments. It will be noted first that the rate of change of resistance is not linear with time. However, an approximation to the curves can be

made with two straight lines, the first having a slope of 22.3 microinches per inch per hour, and the second having a slope of 6.2 microinches per inch per hour. The following is a possible explanation for this phenomenon. The first portion of the curve is primarily a result of corrosion of the wire as obtained at lower temperatures. However, after a period of approximately 120 hours, the metallurgical phase change which occurred at 1000° F under short time conditions now occurs at 800° F. It is believed, therefore, that the second part of the curve having a slope of 6.2 microinches per inch per hour is a result of the combination of the tendency to increase resistance by corrosion and to decrease resistance by the metallurgical phase change. If the test temperature were increased above 800° F, the phase change effect would occur more rapidly, and high rates of decrease of resistance would be encountered.

The rates of zero shift at the various temperatures, shown in figures 6 and 7, have been plotted in figure 8 as a function of temperature. The slope of the initial portion of the 800° F curve is shown plotted and connected by a curve with the slopes determined at 600°, 700°, and 750° F. As mentioned previously, it is believed that this represents predominantly the corrosion of the wire. The slope of the latter portion of the 800° F curve is plotted in figure 8 as a separate point for purposes of comparison.

Resistance to ground and waterproofing. - Shunting a strain gage with high resistances produces a loss in signal output which results in lower indicated strain readings. A discussion of this effect together with a nomograph for quick computation has been presented in appendix IV of reference 2. In the case of high-temperature strain gages, this effect is particularly troublesome because the resistance of the ceramic cements decrease as the temperature is increased. For Quigley 1925, the resistance decreases considerably at temperatures of approximately 1500° F as noted in connection with the dynamic work reported in reference 1. However, for the temperature range of 80° F up to 800° F, measurements made on a series of six gages indicated a relatively constant shunting resistance of approximately 10 megohms. The effect on the gage signal output was, therefore, believed to be negligible.

Quigley 1925 is, however, somewhat hygroscopic. When a gage remains at room temperature in a high-humidity atmosphere, the zero point will shift because of the shunting resistance decrease of the entrapped moisture. Correction is simply effected by heating the gage to 200° or 300° F. In cases where this has been a particular problem, a waterproof coating was applied over the mount, using a material such as Plastilock that has been used satisfactorily at temperatures up to 700° F.

APPARATUS AND TEST PROCEDURE FOR THERMAL STRESS MEASUREMENTS

Stator-Vane Temperature Distribution and Method of Simulation

The turbine stator vane of a particular turbojet engine in the 5000-pound-thrust class was selected for this study because temperature distribution information was readily available. The configuration is shown in figure 9. The stator vane has a span of 3.75 inches and a chord length of 2.81 inches. Seven thermocouples were placed at midspan to determine the chordwise temperature distribution of vane 5 in figure 9. This particular vane is on the centerline of a combustor outlet and, hence, is subjected to higher-temperature operating conditions than those near the combustor-outlet edges. The vanes are precision castings (HS-21 alloy) with a hole through the central portion of each vane for the introduction of the cooling air supplied by the compressor. When the engine is operated at rated speed and temperature (sea level, zero ram), the vane attains an equilibrium chordwise temperature distribution shown in figure 10. The leading and trailing edges operate at temperatures approximately 300° F higher than the midchord region. This would be expected to result essentially in compressive thermal stresses in the leading and trailing edges and tensile thermal stresses in the midchord region.

In order to permit the use of the high-temperature static gages in a determination of the actual thermal stresses produced, it was necessary to duplicate the temperature variations in the vane at a lower base temperature level (average temperature) than exists in the engine. This is due to the maximum useful gage temperature of 800° F as described previously. The average temperature was therefore dropped approximately 1000° F to produce the same temperature variation as exists in the engine but with the leading and trailing edges now at approximately 600° F and the midchord region at approximately 300° F. This procedure does not invalidate the strain measurements unless the elastic limit of the material is exceeded under the actual engine operating conditions, or the value of the expansion coefficient is changed considerably. However, if the measured strains are above the elastic limit at the engine conditions, an indication will still be afforded of the amount of plastic flow taking place. The modulus of elasticity will, of course, be different under the two average temperature conditions, but this can be readily taken into account when converting from strains to stresses.

The duplication of the engine temperature variations in the vane at the lower average-temperature level was accomplished in the apparatus shown schematically in figure 11. The test vane was installed centrally in a 3.25-inch-internal-diameter electric furnace with ducts fastened to each end of the vane to handle the cooling air. In order to duplicate the required temperature pattern in the trailing-edge region, it was found necessary to direct the air at the trailing edge within the hollow vane

by means of a tube having a single row of holes along its length. In the leading-edge region, it was found necessary to add an auxiliary heater (shown in fig. 11) in addition to blocking the heat flow inside the vane by wedging ceramic tubes in the leading edge of the hollow portion. Judicious manipulation of the controls of the main furnace, and the auxiliary leading-edge heater and cooling air enabled a temperature pattern to be produced that was similar to the pattern obtained in the engine.

The instrumented vane, ready for installation in the furnace, is shown in figure 12. The cooling-air-duct work is shown together with the auxiliary heater and thermocouple harness. The thermocouples were iron-constantan (28 gage) with the junctions spot-welded to the external surface of the vane.

Application of Static High-Temperature Strain Gages

Static high-temperature strain gages were mounted on the external surface of the vane at the midspan and positioned chordwise as shown in figure 13. Gage 1 was on the suction side of the vane and 0.25 inch from the leading edge. Gages 2 and 3 were 1.50 inches from the leading edge with gage 2 on the pressure surface and gage 3 on the suction surface. Gage 4 was 0.14 inch from the trailing edge on the suction surface. These positions were selected as probable maximum-stress positions in accordance with preliminary analytical estimates of the thermal stress profile. Initial measurements were made with the active direction of the gages on the longitudinal axis of the vane. A gage length of 3/8 inch was used with a width of 1/16 inch to minimize effects of the steep strain gradients in the chordwise direction.

When the measurements made with the longitudinal gages were compared with the analytically predicted strain values, it was recognized that it would be necessary to have rosette information from each of the gage locations. This is discussed further in the RESULTS section of this report. Consequently, 5/32- by 5/32-inch gages were mounted at each gage position in the transverse direction and, subsequently, in the 45° direction to provide the necessary data for the establishment of the biaxial strain state. A smaller gage length was used in the two latter cases to minimize again the effects of the steep strain gradients in the chordwise direction.

Karma leads of 0.025-inch diameter were used to run from the gages to a point outside the furnace at room temperature. Conversion was then made to copper. The gage factors as shown in figure 5 were modified to take into account the resistance of the lead wires.

Strain Measurement Procedure

After stabilization of the gages as described in a preceding section of this report, the temperature of the vane was slowly raised from 100° to approximately 700° F with the cooling air and the auxiliary heater shut off. In this way, the vane could be heated uniformly with no thermal stresses resulting. During the heating cycle, an accurate record was made of the change in resistance of each gage with temperature in order to furnish a calibration curve to which the subsequent strain readings could be referred. When 700° F was reached, the cooling air and auxiliary heater were turned on, and the desired vane-temperature distribution was obtained. Strain readings at all gage positions were then made, and the cooling air and auxiliary heater shut off. Additional readings were taken while the vane was cooling isothermally, and these values were checked with the original calibration curve to establish the reliability of the gages. The procedure described was carried out at least three times for each of the three different strain-gage installations.

RESULTS AND DISCUSSION

Temperature Distribution

By using the apparatus described previously in this report, a turbine stator vane was subjected to a temperature distribution intended to simulate the chordwise temperature variation under actual engine operating conditions, but with a reduced average temperature. The average temperature was reduced from approximately 1500° to 450° F to make possible the use of the static high-temperature strain gages presently limited to 800° F. As mentioned previously, the reduction of the average temperature would not change the thermal-strain distribution over that obtained in the engine unless the strains were high enough to cause plastic flow. The temperature distribution actually obtained in the test apparatus is shown in figure 14. The test apparatus provided a reasonably good duplication of the engine conditions.

Analytical Determination of Thermal Stresses

Assumptions and description of method. - To provide a basis for correlation of the experimentally measured thermal stresses, an attempt was made to compute the chordwise stress distribution in the vane. The method employed was basically the same as that described in reference 3. It is assumed that the blade does not buckle under the thermal loading and that simple-beam theory is valid for such a shape. In addition, on the basis of information presented in reference 4, the effect of spanwise temperature variations on the spanwise stress distribution was neglected. It was shown in reference 4, for example, that spanwise temperature variations of as

much as 30 percent from one end of the vane to the other would have a negligible effect. The spanwise temperature variation obtained in the test apparatus was less than this value.

The method used converts the thermal problem to an external loading problem. The chordwise temperature distribution chosen for the computation was (fig. 14) obtained from the test apparatus, and the cross-sectional dimensions of the vane were obtained by precision measurements of the same vane as used in the experimental stress determination. If E and α are both taken to be functions of temperature, the external loading at point P' in figure 15 is then E_P, α_P, T_P, and the desired stress at point P is

$$\sigma_{z,P} = -E_P\alpha_P T_P + \frac{\int_A E\alpha T \ dA}{A} + y_P \frac{\int_A E\alpha Ty \ dA}{I_{xx}} + x_P \frac{\int_A E\alpha Tx \ dA}{I_{yy}} \tag{1}$$

where I_{xx} and I_{yy} are the moments of inertia about the principal axes. In order to calculate the stress distribution σ_z, the principal axes of inertia must first be determined and then the moments of inertia about these axes. The method of reference 5 was used for this purpose. The integrals in equation (1) were evaluated by subdividing the blade cross-sectional area A into a number of smaller areas dA as shown in figure 15, by evaluating $E_i\alpha_i$ and T_i at the center of dA, and by letting

$$\int_A E\alpha T \ dA = \sum_{i=1}^{n} \bar{E}_i\bar{\alpha}_i\bar{T}_i \ dA_i$$

and

$$\int_A E\alpha Ty \ dA = \sum_{i=1}^{n} \bar{E}_i\bar{\alpha}_i\bar{T}_i\bar{y}_i \ dA_i$$

and

$$\int_A E\alpha Tx \ dA = \sum_{i=1}^{n} \bar{E}_i\bar{\alpha}_i\bar{T}_i\bar{x}_i \ dA_i$$

where n is the total number of small areas used in the subdivision, and the bars over the letters denote the average value in the small area. These summations are evaluated and by letting

$$\frac{\sum_{i=1}^{n} \bar{E}_i\bar{\alpha}_i\bar{T}_i \ dA_i}{A} = C_1$$

and

$$\frac{\sum_{i=1}^{n} \bar{E}_i \bar{\alpha}_i \bar{T}_i \bar{y}_i \, dA_i}{I_{xx}} = C_2$$

and

$$\frac{\sum_{i=1}^{n} \bar{E}_i \bar{\alpha}_i \bar{T}_i \bar{x}_i \, dA_i}{I_{yy}} = C_3$$

$\sigma_{z,p}$ can be evaluated as

$$\sigma_{z,p} = -E_p \alpha_p T_p + C_1 + C_2 y_p + C_3 x_p$$

Computed stress distribution. - Through use of the method outlined previously, the stresses in the spanwise or z direction were computed, and their variation in the chordwise direction is shown in figure 16. The stresses shown are those which would exist at the outside surface of the vane. On the pressure surface, the thermal stress reaches a peak value of 31,000 psi in tension at approximately midchord. The trailing-edge region is in compression at a peak value of about 24,500 psi. The leading-edge region being quite blunt has a wide stress variation from 8000 psi in tension to 27,000 psi in compression. The suction surface, although being predominantly in compression, goes into tension in the midchord region by a value of 10,500 psi.

Experimental Stress Measurements

Thermal stress measurements at four different locations on the external surface of the stator vane were made using static high-temperature strain gages and the test apparatus previously described. In the first measurements, the gages were alined in the direction of the longitudinal axis of the vane in order to obtain data that could be directly compared with the analytical results shown in figure 16. When these measurements were obtained, however, they were in poor agreement with the analysis. It was suspected that a contributing source of the difficulty was involved in the simple-beam-theory assumption that plane sections remain plane and, therefore, a room-temperature test was devised to determine the principal strain directions on both surfaces when the vane was subjected to a bending moment about the x-axis. The ends of the vane were fastened to grips which permitted a bending moment to be applied through the use of weights placed on one of the grips. Deflection measurements of the

leading and trailing edges of the vane showed the absence of torsion loading. A strain rosette was mounted on both the suction and pressure surfaces at a location identified by the intersection of the midchord and midspan lines. The results of the test indicated a difference of 20° between the principal directions on the two sides of the vane at the particular gage location chosen, thus violating one of the main assumptions of the analysis.

As a result of the findings of the simple-bending test, high-temperature static strain gages were also mounted at each of the four locations in the transverse direction and also at 45° to the longitudinal direction in order to provide a complete picture of the biaxial strain state in the vane. The results are shown in figure 17. The values of the maximum and minimum principal stresses are given at each of the four gage locations in addition to the deviation of the maximum principal stress directions from the longitudinal axis. The leading and trailing edges are in compression with the maximum principal stresses of -18,100 and -27,200 psi, respectively. In both cases, the directions of the maximum principal stresses deviate from the longitudinal axis by at least 20°. At gage 2 on the pressure surface, a maximum principal stress of 26,200 psi was obtained with the principal direction 19° from the longitudinal axis. At gage 3 on the suction surface, a maximum principal stress of -19,600 psi was obtained with the principal direction 7° from the longitudinal. To depict the relation between the analytical and experimental results, the values for the maximum principal stresses at the four gage locations are plotted on the graph shown in figure 16. In spite of the limitations of the analytical procedure, the values of the stresses predicted in the longitudinal direction compare favorably with the maximum principal stresses at three of the four gage locations. At the midchord position on the suction surface there is a difference of approximately 18,000 psi. The differences between the analytical and experimental results are believed to be a result of the assumption in the analytical procedure that plane sections remain plane.

4715

SUMMARY OF RESULTS

The thermal stresses in a turbojet turbine stator vane were measured through the use of a static high-temperature strain gage developed during the investigation. The temperature variation in the vane as measured in the engine at rated operating conditions was duplicated in a test setup at a lower average temperature to permit the use of the gages limited to approximately 800° F. The same thermal strains were obtained in the vane in the test setup as in the engine. Strain measurements were made in four locations: leading edge, trailing edge, and midchord on both the suction and pressure surfaces.

The maximum principal stresses measured in the leading- and trailing-edge locations were in compression and were 18,100 and 27,200 psi, respectively. At the midchord location on the suction surface, the maximum principal stress was found to be 19,600 psi in compression, and at the midchord on the pressure surface was found to be 26,200 psi in tension. Considerable deviation of the maximum principal stress directions from the longitudinal axis was found in all four locations, making a direct comparison with analytical results rather tenuous because of limiting assumptions of simple beam theory. Therefore, it might be expected that the experimental and analytical results would not necessarily be in agreement. In this particular case, it was found that at three out of the four gage locations the measured values were close to the theoretical while a large difference was noted at the fourth location.

The gage developed for measuring static strains at temperatures up to 800° F utilizes Karma wire as the strain-sensitive element and is bonded to the test structure with Quigley 1925 ceramic coating. Gage factors for three gage sizes were determined under static loading conditions at temperatures up to 800° F. The 1/4- by 1/4-inch gage, for example, had a gage factor of 2.16 at room temperature, dropping to 1.93 at 800° F. The zero shift as a function of the many variables which affect the absolute resistance of the gage was below 1.2 microinches per inch per hour at temperatures below 600° F. At 750° F the zero shift was 5.8 microinches per inch per hour.

Lewis Flight Propulsion Laboratory
National Advisory Committee for Aeronautics
Cleveland, Ohio, November 27, 1957

REFERENCES

1. Kemp, R. H., Morgan, W. C., and Manson, S. S.: Advances in High-Temperature Strain Gages and Their Application to the Measurement of Vibratory Stresses in Hollow Turbine Blades During Engine Operation. Proc. Soc. Exp. Stress Analysis, vol. VIII, no. 2, 1951, pp. 209-228.

2. Palermo, P. M.: Methods of Waterproofing SR-4 Strain Gages. Proc. Soc. Exp. Stress Analysis, vol. XIII, no. 2, 1956, pp. 79-83.

3. Timoshenko, S., and Goodier, J. N.: Theory of Elasticity. Second ed., McGraw-Hill Book Co., Inc., 1951.

4. Mendelson, Alexander, and Hirschberg, Marvin: Analysis of Elastic Thermal Stresses in Thin Plate with Spanwise and Chordwise Variations of Temperature and Thickness. NACA TN 3778, 1956.

5. Gendler, Sel, and Johnson, Donald F.: Determination of Minimum Moments of Inertia of Arbitrarily Shaped Areas, Such as Hollow Turbine Blades. NACA RM E9H10, 1950.

TABLE I. - CHARACTERISTICS OF STRAIN-GAGE WIRES

Alloy	Specific resistivity, $\frac{\text{ohm}}{\text{cir. mil-ft}}$	Approximate gage-sensitivity factor	Average temperature coefficient of resistance of sample gages on HS-21 alloy, microin./(in./^{o}F)
Advance	294	2	[a]4
Nichrome V	650	2	[b]30
80-Percent platinum - 20-percent iridium	200	6	[b]80
Karma	800	2	[b]-2.5

[a]100° to 400° F.

[b]100° to 800° F.

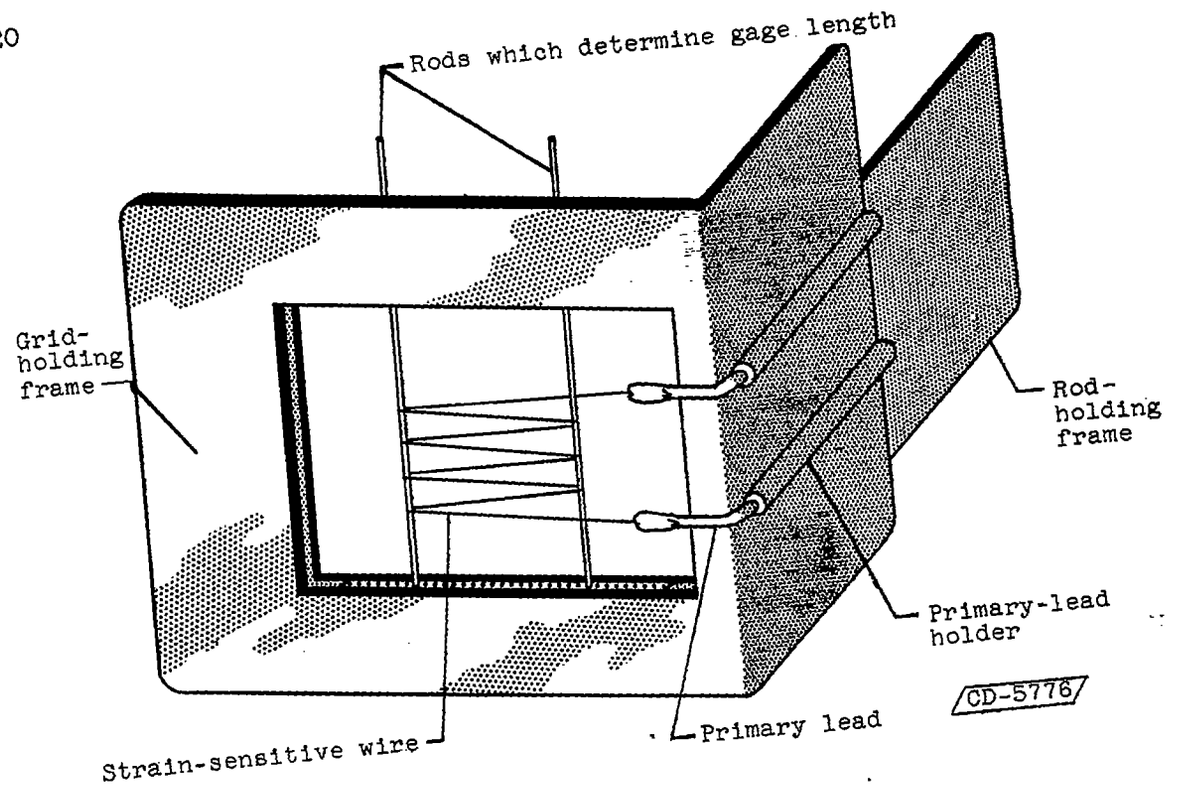

(a) First step.

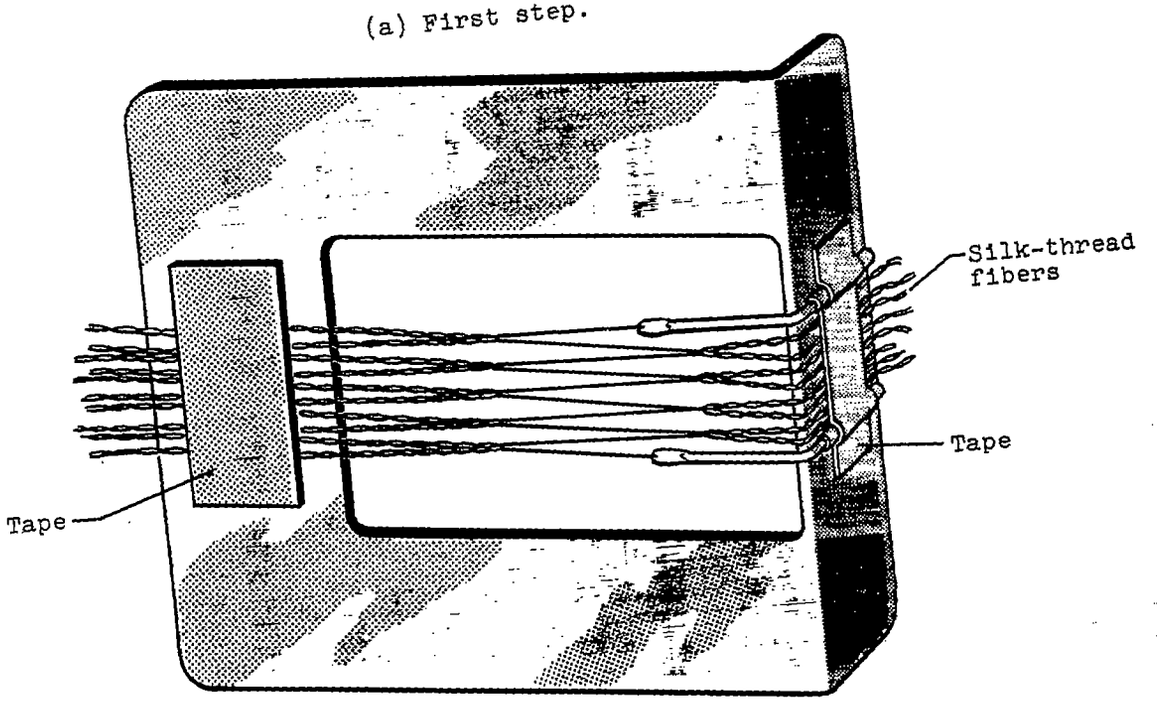

(b) Final step.

Figure 1. - Preparation of strain-gage grid.

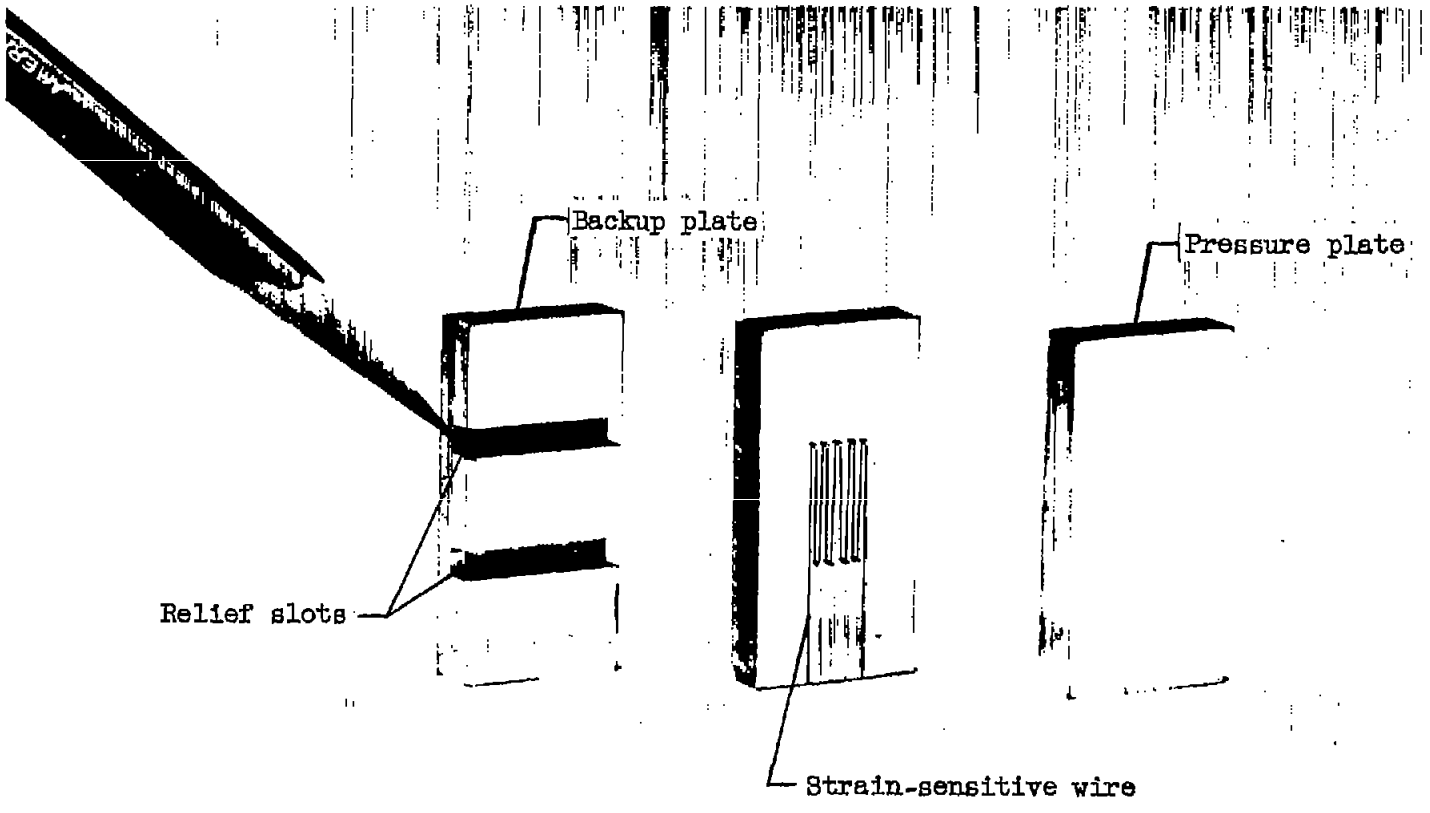

Figure 2. - Jig for preforming gage grid by pressure method.

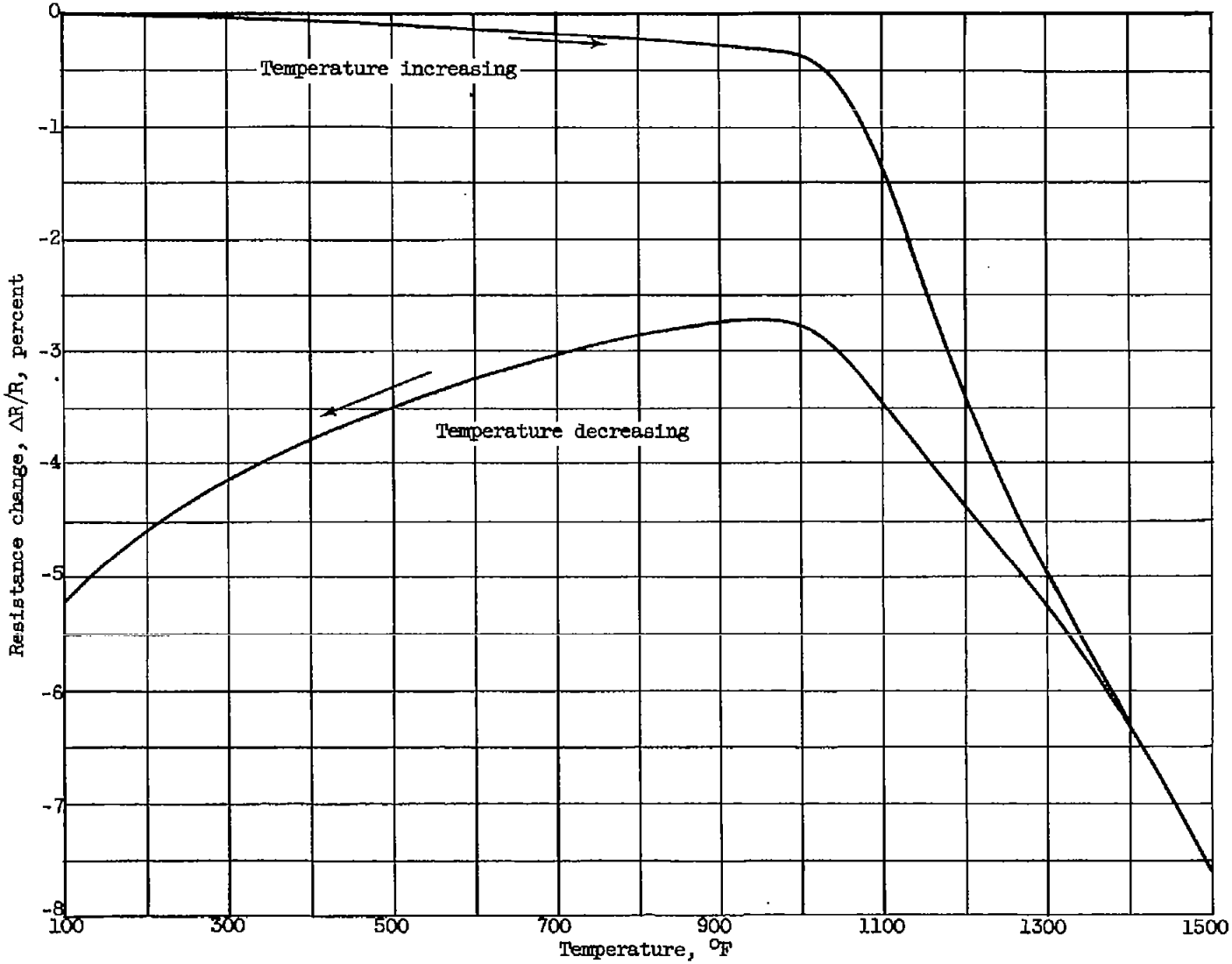

Figure 3. - Variation of resistance with temperature for a mounted Karma gage.

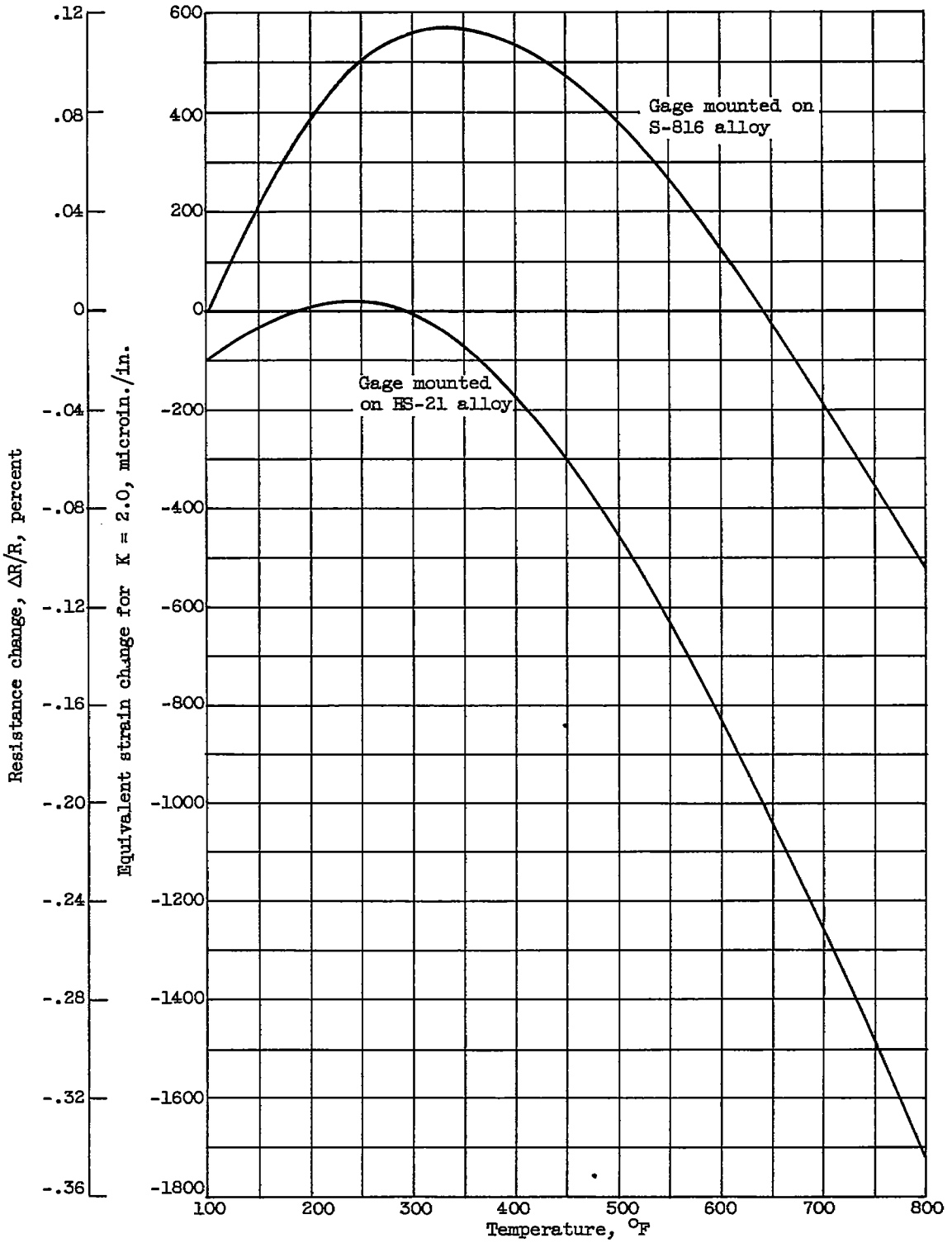

Figure 4. - Resistance variation of mounted Karma gages up to 800° F using the wire in the as-received condition.

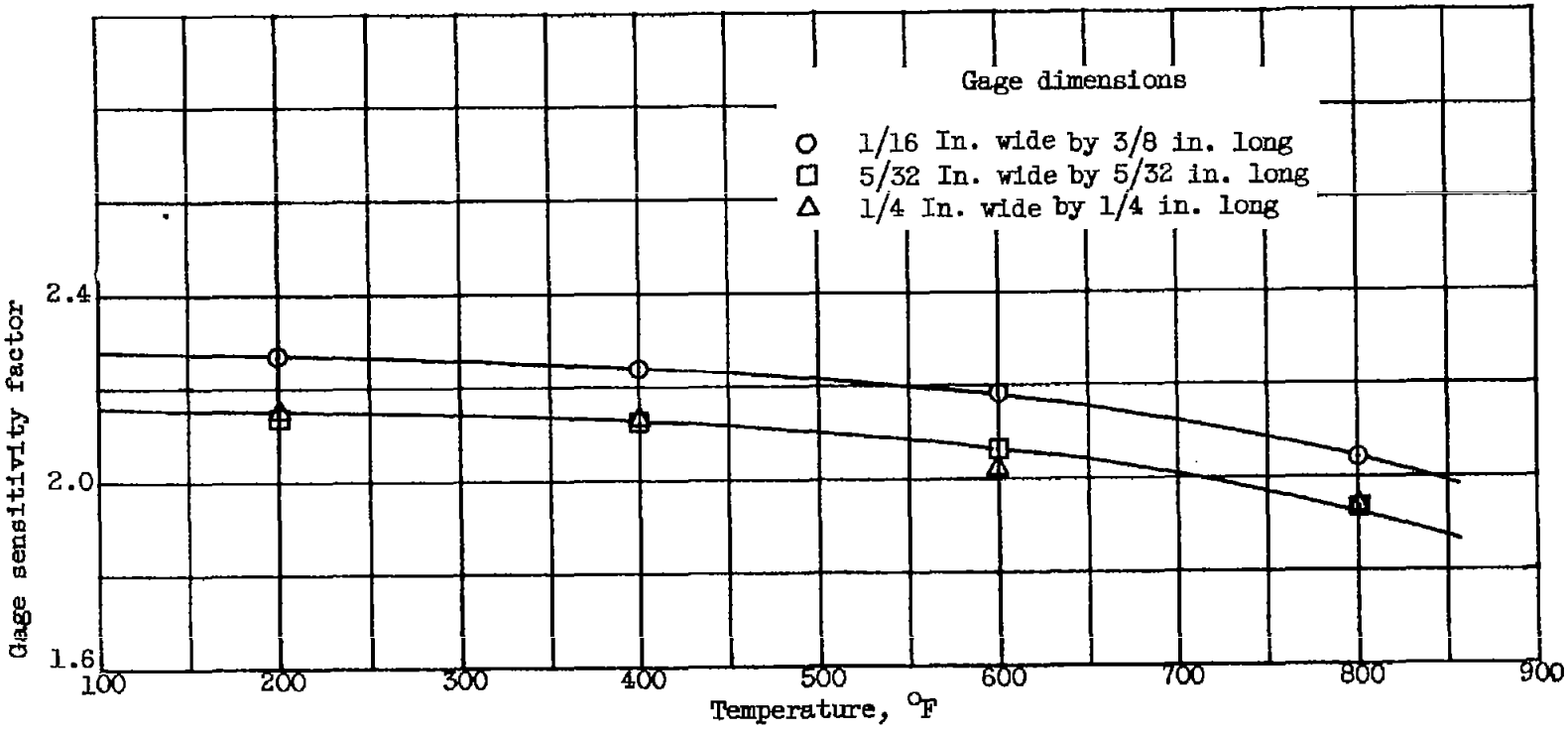

Figure 5. - Gage sensitivity factor variation with temperature.

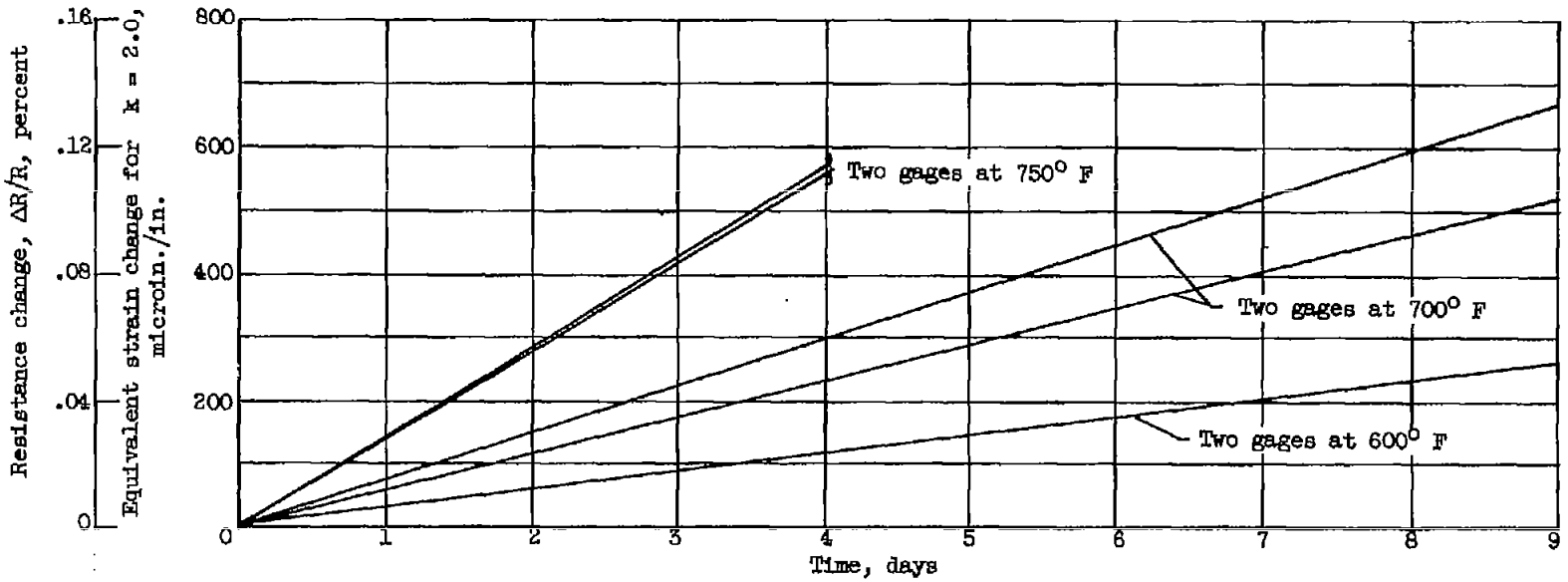

Figure 6. - Zero shift with time for Karma gages at temperatures of 600°, 700°, and 750° F.

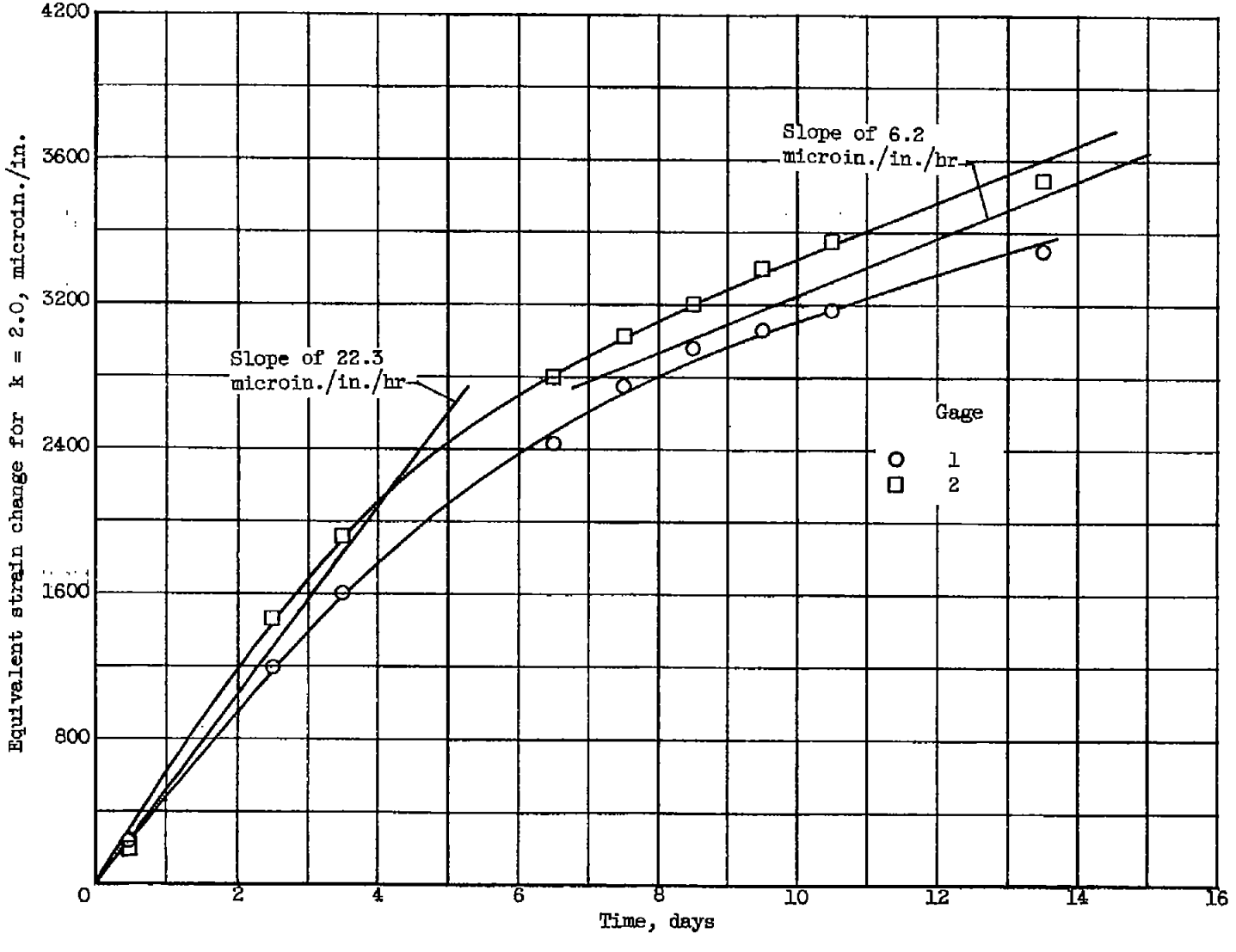

Figure 7. - Zero shift with time for two Karma gages at 800° F.

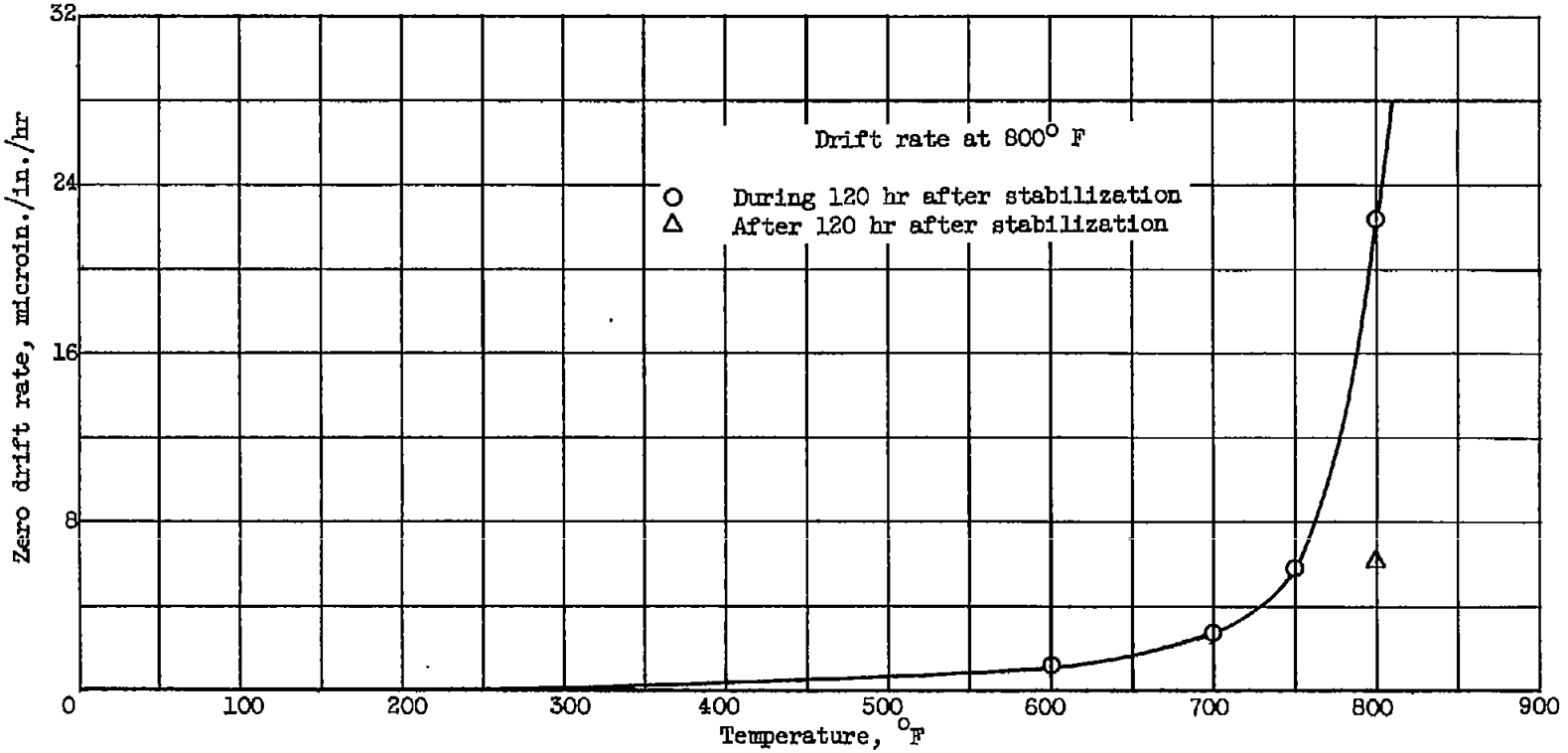

Figure 8. - Variation of zero drift rate with temperature for Karma gages.

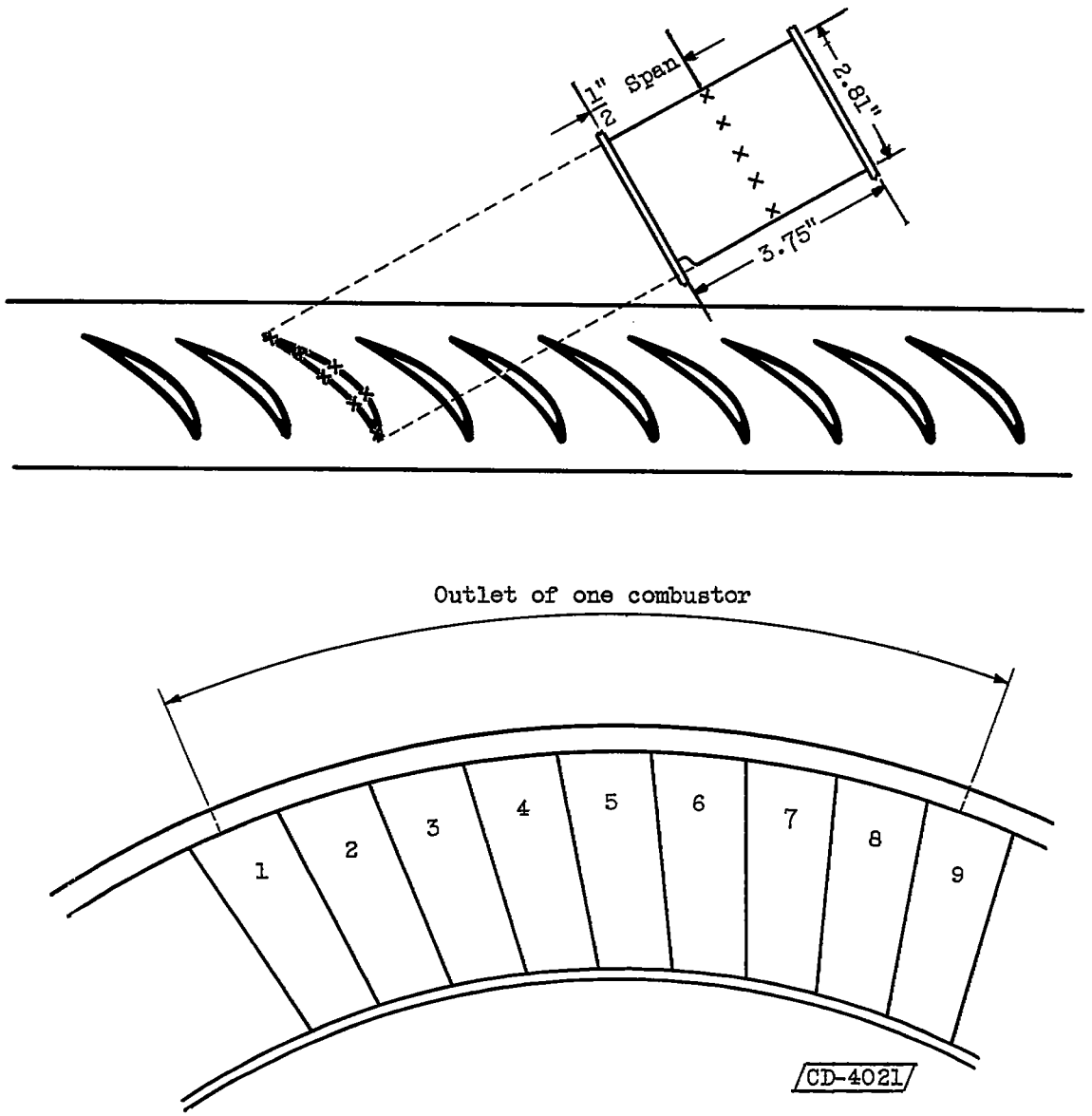

Figure 9. - Turbine-stator-vane configuration.

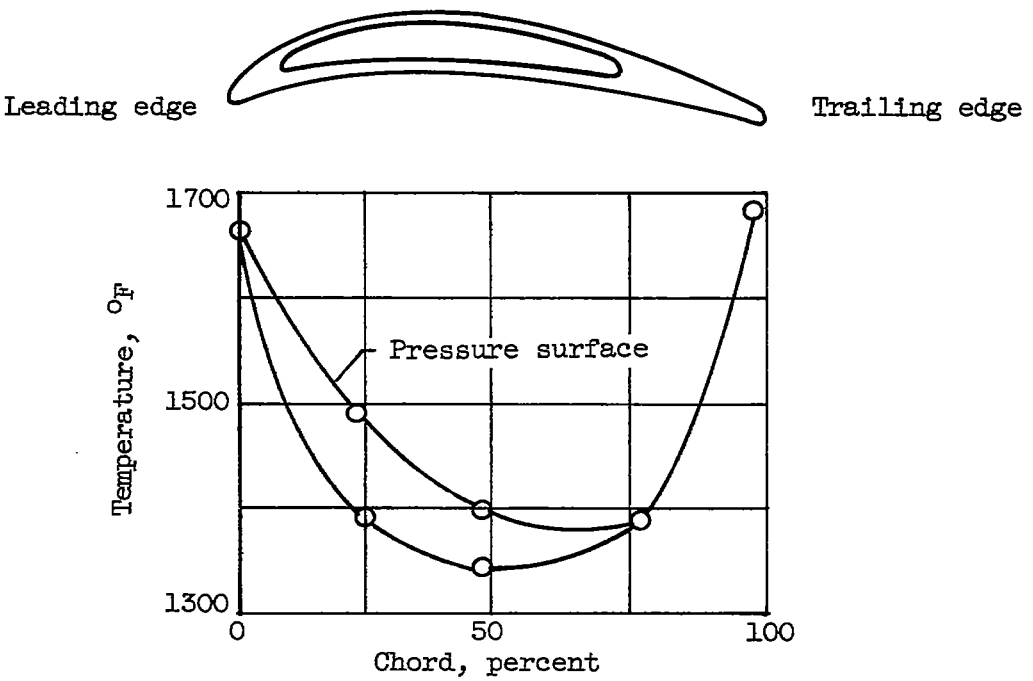

Figure 10. - Chordwise temperature distribution in turbine stator vane of turbojet.

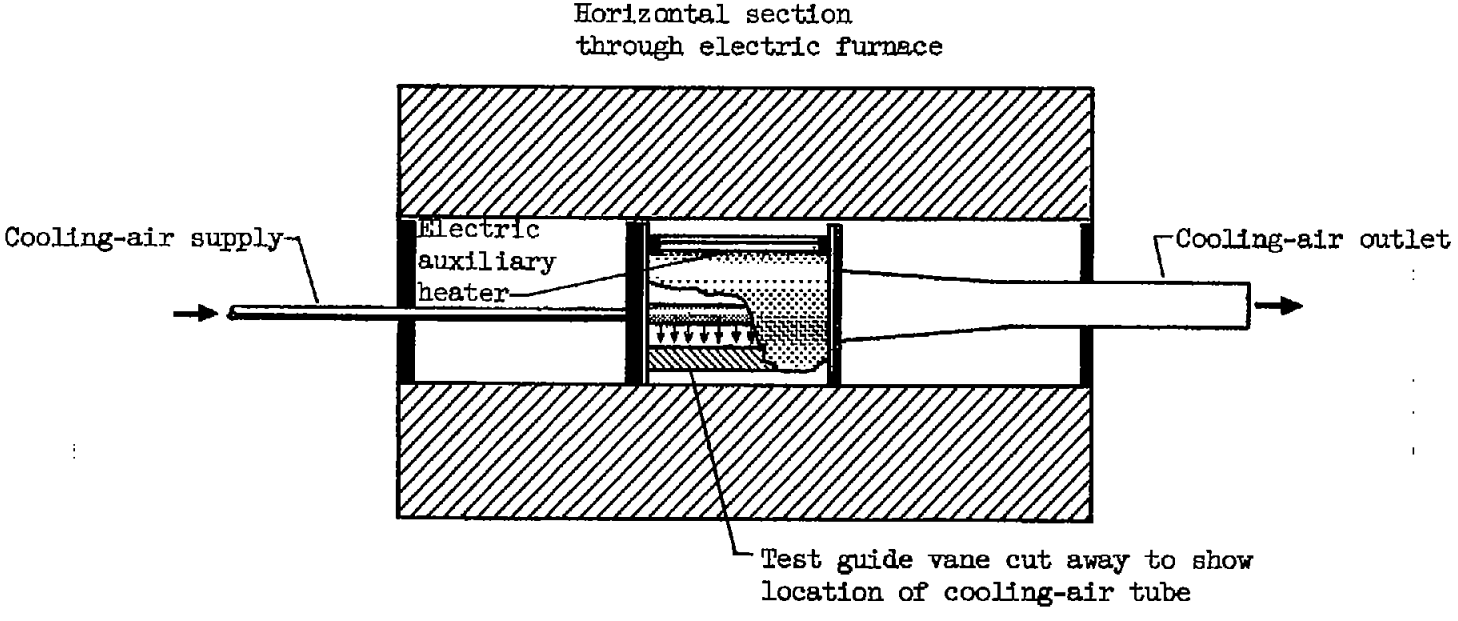

Figure 11. - Schematic drawing of apparatus for producing temperature gradients in turbine stator vane.

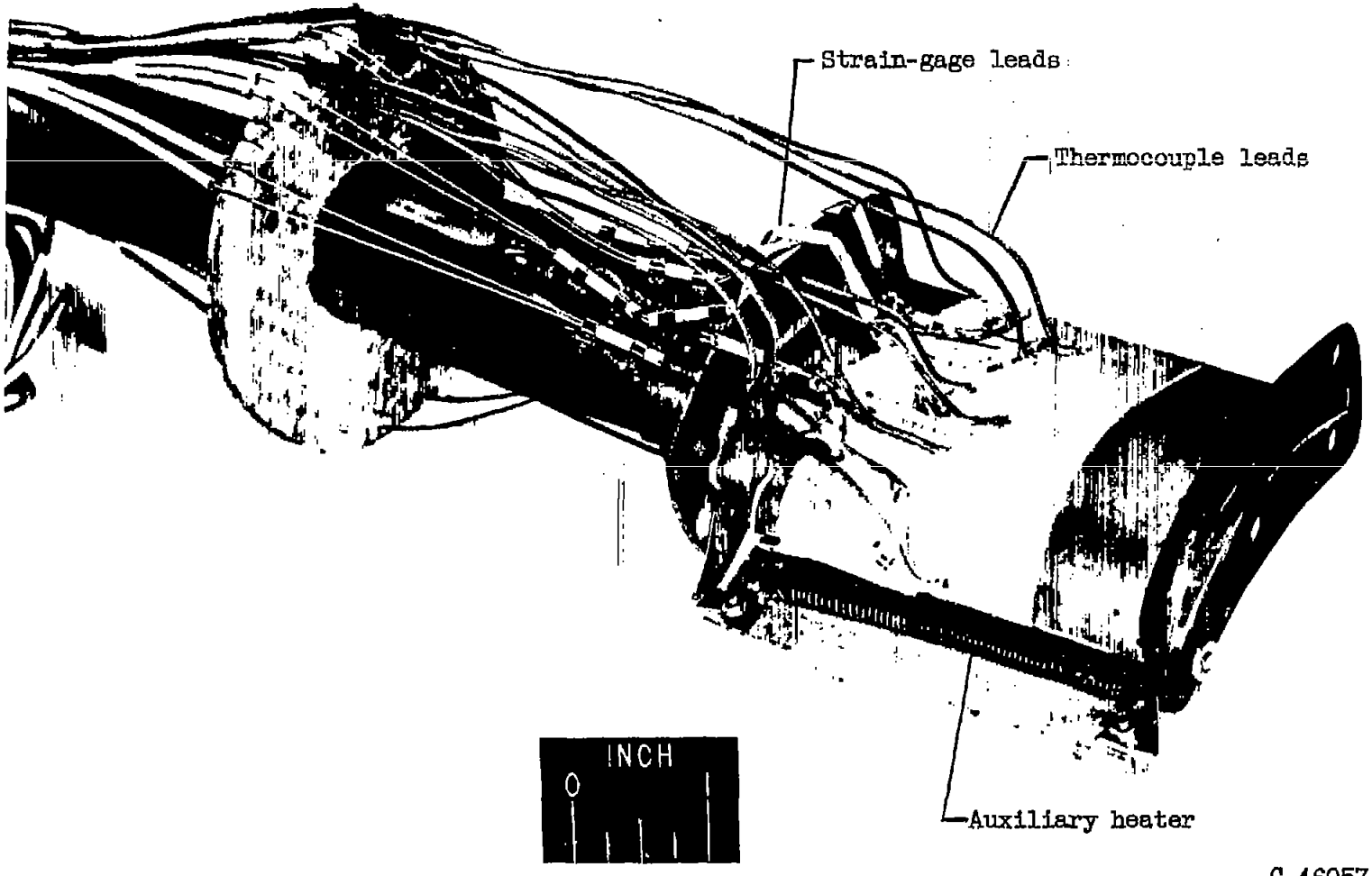

Figure 12. - Instrumented vane ready for installation in furnace.

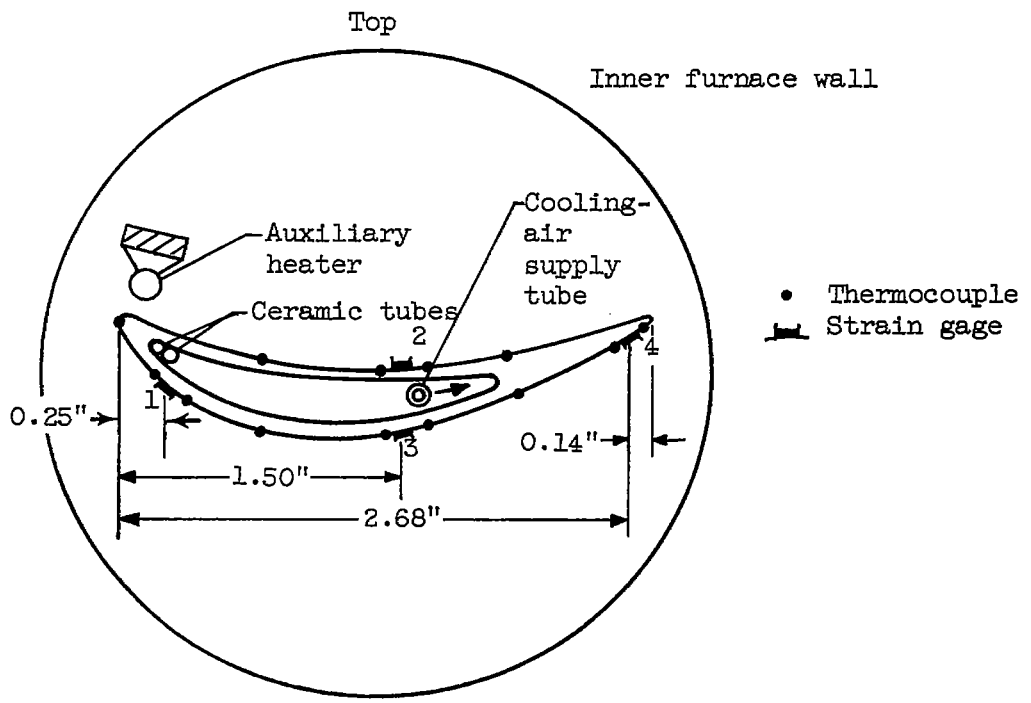

Figure 13. - Location of static high-temperature strain gages on vane.

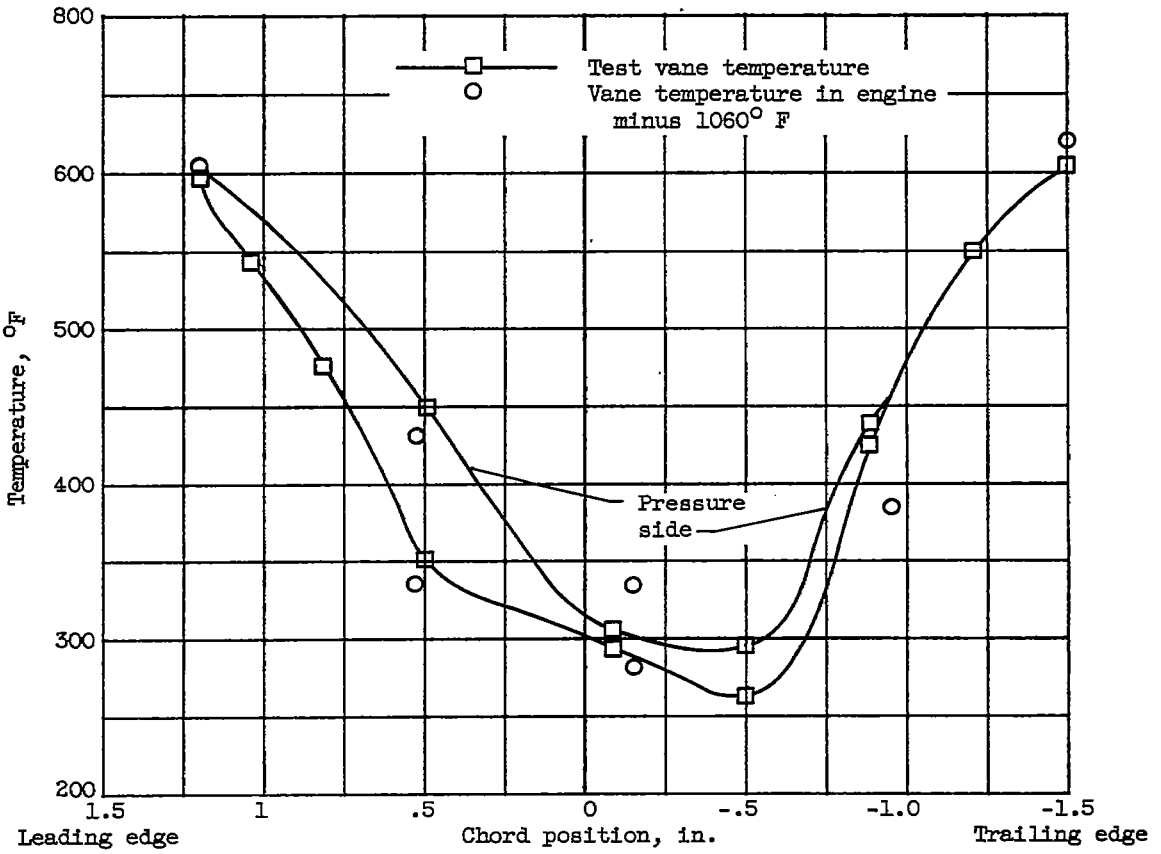

Figure 14. - Chordwise temperature distribution in vane obtained in test apparatus.

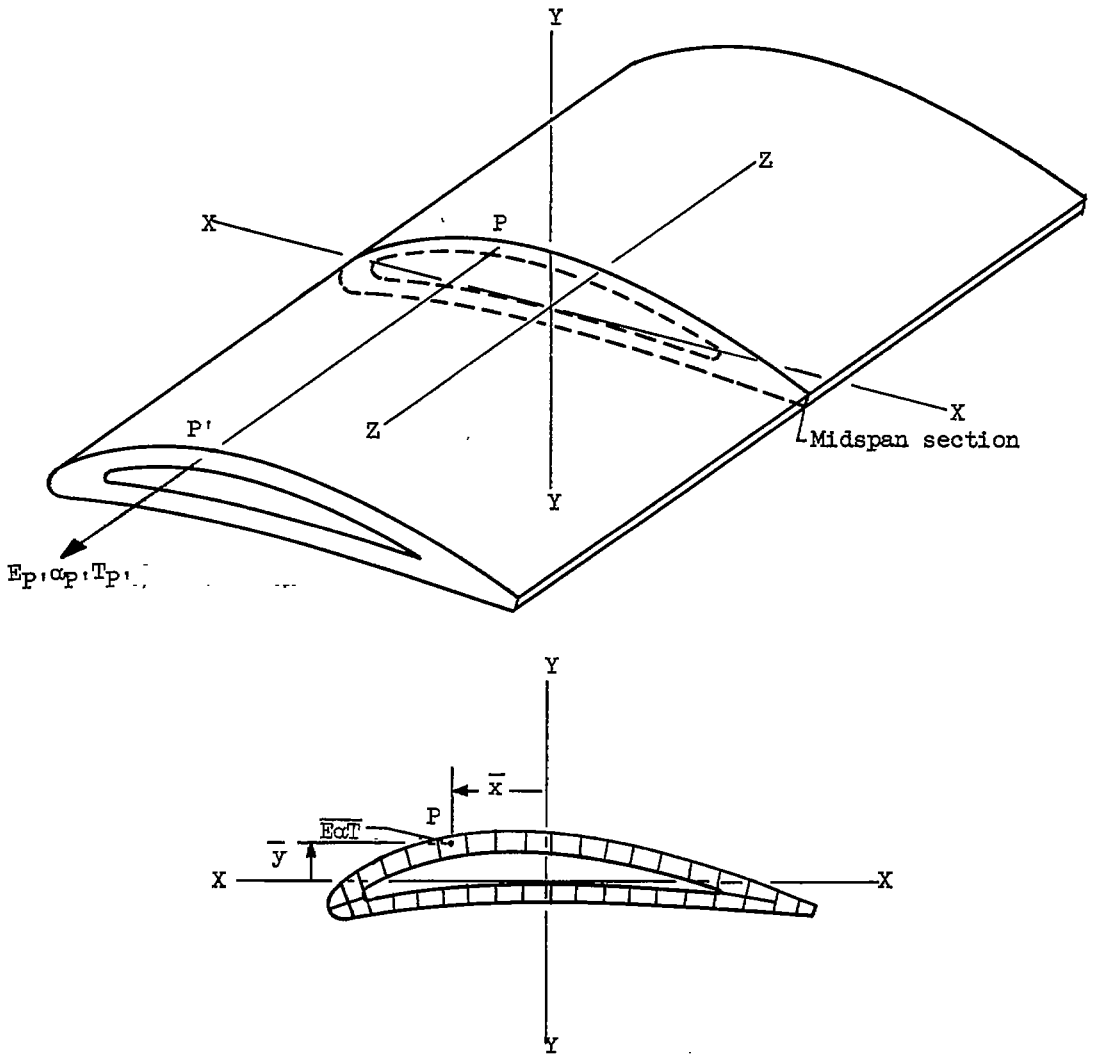

Figure 15. - Schematic view of turbine stator vane illustrating analytical method of determination of thermal stresses.

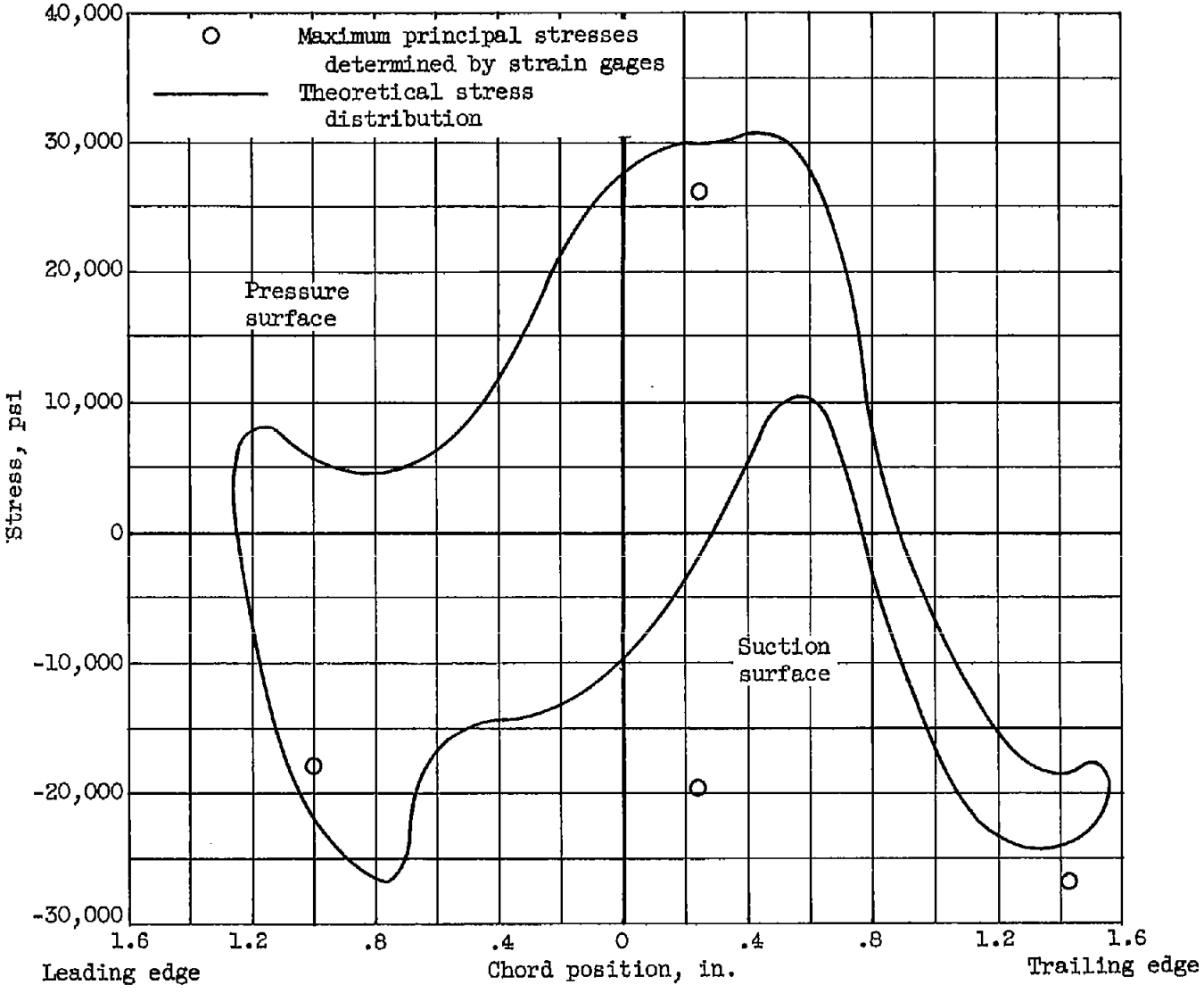

Figure 16. - Thermal stresses in turbine stator vane.

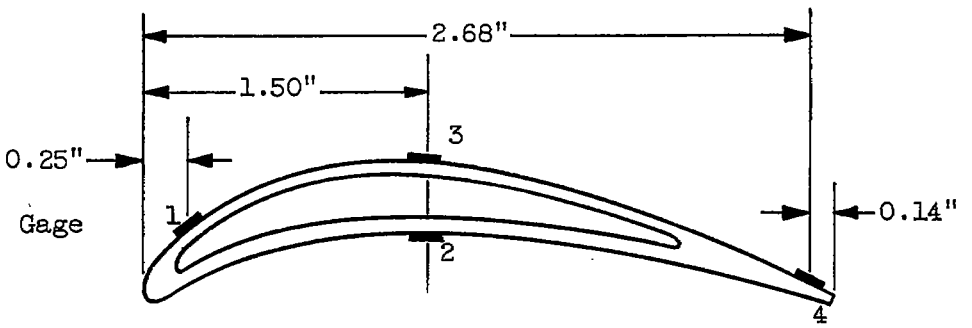

Gage location	Maximum principal stress, psi	Minimum principal stress, psi	Deviation of maximum principal stress direction from spanwise axis viewed from suction surface, deg
1	-18,100	-9,200	22 Clockwise
2	26,200	10,500	19 Clockwise
3	-19,600	-11,100	7 Clockwise
4	-27,200	1,930	$24\frac{1}{2}$ Counterclockwise

Figure 17. - Principal stresses and directions determined by high-temperature strain gages in turbine stator vane.